remote sensing

MDPI

Supplementary Material

Crustal Deformation on the Northeastern Margin of the Tibetan Plateau from Continuous GPS Observations

Xiaoning Su [1,2], Lianbi Yao [1,*], Weiwei Wu [2], Guojie Meng [2], Lina Su [3], Renwei Xiong [2] and Shunying Hong [2]

[1] College of Surveying and Geo-informatics, Tongji University, Shanghai 200092, China; suxiaoning_666@126.com (X.S.)
[2] Key Laboratory of Earthquake Prediction, Institute of Earthquake Forecasting, China Earthquake Administration, Beijing 100036, China; 14_jasonwu@tongji.edu.cn (W.W.); guojiemeng@126.com (G.M.); xiong@ief.ac.cn (R.X.); hongshunying@cea-ies.ac.cn (S.H.)
[3] Shaanxi Earthquake Agency, Xi'an 710068, China; sulinawhu@163.com
* Correspondence: lianbi@tongji.edu.cn; Tel.: +86-021-6598-4460

Received: 25 November 2018; Accepted: 23 December 2018; Published: 26 December 2018

Abstract: We installed 10 continuous Global Positioning System (GPS) stations on the northeast margin of the Tibetan Plateau at the end of 2012, in order to qualitatively investigate strain accumulation across the Liupanshan Fault (LPSF). We integrated our newly built stations with 48 other existing GPS stations to provide new insights into three-dimensional tectonic deformation. We employed white plus flicker noise model as a statistical model to obtain realistic velocities and corresponding uncertainties in the ITRF2014 and Ordos-fixed reference frame. The total velocity decrease from northwest to southeast in the Longxi Block (LXB) was 5.3 mm/yr within the range of 200 km west of the LPSF on the horizontal component. The first-order characteristic of the vertical crustal deformation was uplift for the northeastern margin of the Tibetan Plateau. The uplift rates in the LXB and the Ordos Block (ORB) were 1.0 and 2.0 mm/yr, respectively. We adopted an improved spherical wavelet algorithm to invert for multiscale strain rates and rotation rates. Multiscale strain rates showed a complex crustal deformation pattern. A significant clockwise rotation of about 30 nradians/yr (10^{-9} radians/year) was identified around the Dingxi. Localized strain accumulation was determined around the intersectional region between the Haiyuan Fault (HYF) and the LPSF. The deformation pattern across the LFPS was similar to that of the Longmengshan Fault (LMSF) before the 2008 Wenchuan M_S 8.0 earthquake. Furthermore, according to the distributed second invariant of strain rates at different spatial scale, strain partitioning has already spatially localized along the Xiaokou–Liupanshan–Longxian–Baoji fault belt (XLLBF). The tectonic deformation and localized strain buildup together with seismicity imply a high probability for a potential earthquake in this zone.

Keywords: northeastern margin of Tibetan Plateau; continuous GPS observations; time series analysis; three-dimensional velocity field; strain partitioning; crustal uplift

---

Table S1. Three dimensional GPS velocities in ITRF2014 reference frame and horizontal GPS velocities in Ordos-fixed reference (in mm/yr) together with associated one-sigma uncertainties that have been estimated by using a combined noise model of white plus flicker noise.

Station	Longitude	Latitude	ITRF2014 (mm/yr)			Stable Ordos		Uncertainty (one-sigma)		
	(°)	(°)	Ve	Vn	Vu	Ve	Vn	Se	Sn	Su
BYJY	104.69	36.57	37.28	-5.65	2.34	3.98	3.71	0.94	0.73	1.42
GNDB	103.23	34.06	37.18	-4.84	2.22	2.56	4.58	0.81	0.67	1.31
GNYL	103.66	34.96	37.17	-4.64	-0.88	3.01	4.76	1.00	0.56	1.46
GSDX	104.60	35.55	35.79	-6.84	0.11	2.00	2.52	0.22	0.24	0.35
GSJN	105.76	35.53	33.88	-8.45	0.96	0.18	0.86	0.23	0.26	0.37
GSJT	104.06	37.18	34.48	-5.48	0.46	1.41	3.90	0.23	0.26	0.28
GSLX	104.65	35.00	35.04	-7.07	0.78	0.99	2.29	0.23	0.24	0.40
GSMX	104.02	34.43	37.22	-5.80	0.45	2.85	3.59	0.26	0.28	0.39
GSPL	106.59	35.55	33.99	-9.45	0.54	0.38	-0.18	0.23	0.24	0.40
GSQS	106.21	34.75	32.90	-8.66	-1.02	-1.12	0.63	0.25	0.26	0.43
GSTS	105.91	34.48	34.20	-8.54	-0.11	0.03	0.77	0.26	0.28	1.04
GSWD	104.82	33.42	34.73	-8.15	-0.82	-0.03	1.20	0.25	0.26	0.41
LNHX	106.07	33.72	34.98	-8.22	-3.31	0.47	1.08	0.96	0.61	1.35
LNKX	105.59	33.33	33.79	-7.84	1.42	-0.94	1.48	0.91	0.76	1.40
LNLB	105.07	34.32	35.25	-7.82	0.51	0.92	1.52	0.94	0.63	1.66
LP01	105.18	36.06	36.25	-6.80	-1.99	2.75	2.54	0.37	0.37	0.49
LP02	105.61	35.97	35.68	-9.38	1.38	2.18	-0.06	0.38	0.41	0.47
LP03	105.81	35.96	35.25	-9.71	1.02	1.76	-0.40	0.40	0.38	0.49
LP04	105.96	35.95	35.01	-9.40	1.40	1.53	-0.10	0.40	0.35	0.58
LP05	106.10	35.92	34.91	-8.68	-1.82	1.43	0.62	0.37	0.42	0.91
LP06	106.24	35.92	34.12	-8.84	1.52	0.65	0.45	0.37	0.38	0.51
LP07	106.45	35.86	33.83	-9.26	2.25	0.35	0.02	0.36	0.38	0.50
LP08	106.65	35.81	33.46	-8.57	-0.73	-0.02	0.70	0.35	0.40	0.86
LP09	105.93	36.28	35.27	-7.85	1.03	1.95	1.46	0.42	0.37	0.47
LP10	105.69	36.28	35.47	-8.60	1.16	2.13	0.72	0.39	0.41	0.52
NXHY	105.65	36.55	34.13	-6.79	-1.30	0.91	2.53	0.22	0.23	0.31
NXZW	105.24	37.59	32.65	-5.74	0.41	-0.10	3.60	0.22	0.23	0.27
QYNX	107.92	35.51	33.41	-10.03	2.22	-0.09	-0.82	0.94	0.66	1.66
QYSC	107.03	36.96	32.24	-8.48	2.47	-0.65	0.77	0.93	0.54	1.49
QYTQ	107.44	36.10	33.33	-9.21	3.73	0.07	0.02	1.02	0.62	1.50
SNFG	107.40	34.58	34.91	-7.79	2.51	0.92	1.45	0.31	0.33	0.58
SNFX	106.51	33.91	34.41	-11.28	-0.37	0.03	-2.00	0.29	0.38	0.69
SNHX	108.50	34.16	36.13	-8.62	-5.63	2.04	0.56	0.32	0.33	0.58
SNJY	108.75	34.70	33.92	-10.45	0.54	0.11	-1.28	0.33	0.24	0.75
SNLX	106.61	34.70	34.28	-9.05	1.18	0.27	0.22	0.29	0.29	0.48
SNTB	107.32	34.06	34.66	-9.77	0.65	0.42	-0.53	0.24	0.26	0.37
SNXY	108.39	35.17	33.72	-9.39	1.08	0.10	-0.21	0.22	0.23	0.34
SNYL	108.02	34.31	35.36	-9.56	0.32	1.30	-0.36	0.30	0.28	0.49
SNYX	107.62	33.37	34.34	-10.03	1.11	-0.19	-0.81	0.29	0.33	0.44

YANC	107.44	37.78	32.38	-9.10	0.51	-0.06	0.13	0.21	0.21	0.42
GNXH	102.51	35.20	37.79	-2.42	1.69	3.63	7.02	1.23	1.07	2.02
GSGL	102.89	37.45	33.99	-4.87	0.95	0.94	4.56	0.25	0.27	0.55
GSMA	102.06	34.02	40.74	-4.36	-0.02	6.00	5.10	0.23	0.26	0.41
GSML	100.82	38.44	32.55	-3.21	0.20	-0.23	6.29	0.26	0.26	0.39
GSMQ	103.09	38.63	33.85	-5.73	-0.12	1.40	3.69	0.38	0.33	0.43
JCYC	102.01	38.24	31.06	-4.67	0.48	-1.69	4.79	0.96	0.49	1.26
LZLC	102.86	36.56	37.09	-0.92	0.74	3.61	8.51	0.92	0.87	1.14
NXYC	106.27	38.49	31.97	-7.63	-3.57	-0.22	1.66	0.25	0.26	0.50
QHGC	100.13	37.33	36.91	-2.09	-0.34	3.53	7.43	0.27	0.30	0.35
QHME	101.40	37.47	36.91	-3.08	0.21	3.72	6.40	0.24	0.26	0.32
QHMQ	100.25	34.48	41.42	-1.44	-0.34	6.72	8.08	0.23	0.25	0.37
QHQL	100.24	38.19	33.91	-3.27	1.03	0.95	6.25	0.25	0.26	0.56
QHTR	102.01	35.52	37.48	-1.97	0.85	3.42	7.49	0.28	0.38	0.94
RURG	102.96	33.58	40.23	-6.83	-1.49	5.37	2.60	0.35	0.38	1.22
SNLT	109.28	34.34	33.33	-9.59	0.60	-0.61	-0.45	0.28	0.30	0.47
SNZA	109.16	33.43	33.90	-10.19	0.20	-0.47	-1.05	0.29	0.30	0.48
XIAA	108.99	34.18	31.15	-8.29	-4.93	-2.89	0.86	0.19	0.13	0.49
XNIN	101.77	36.60	38.40	-4.45	0.89	4.83	5.02	0.14	0.12	0.30

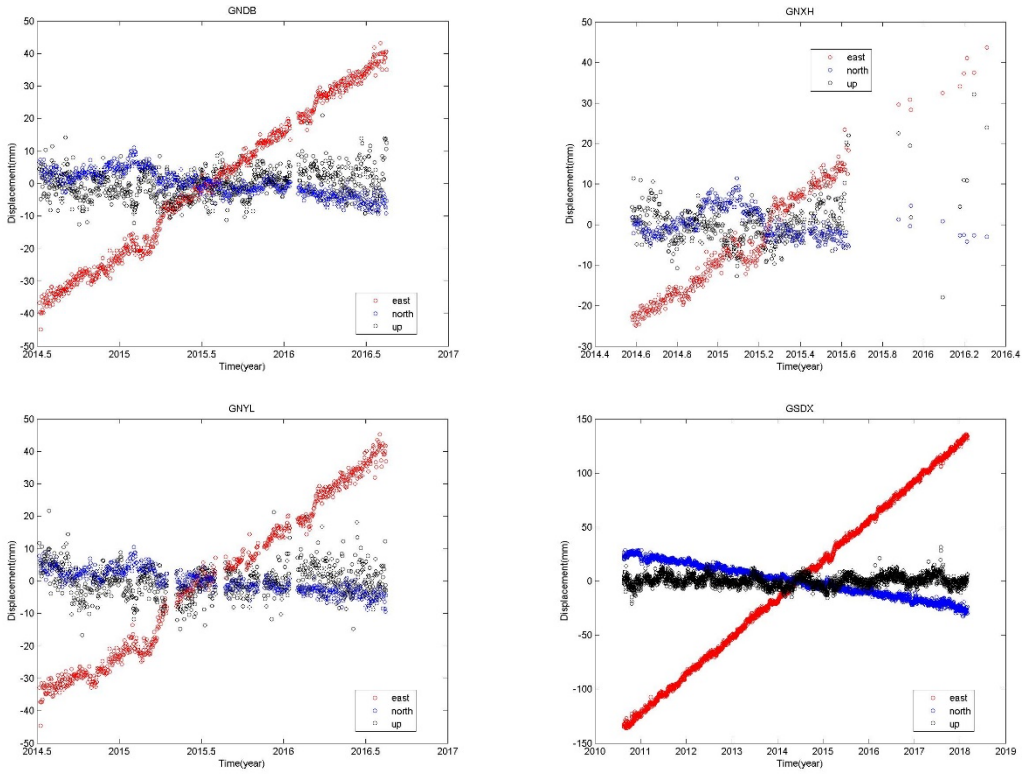

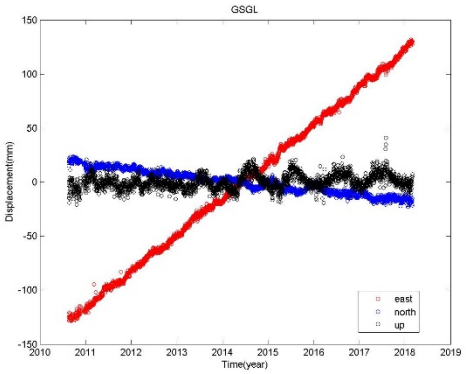
GSGL
Displacement(mm)
Time(year)
east
north
up

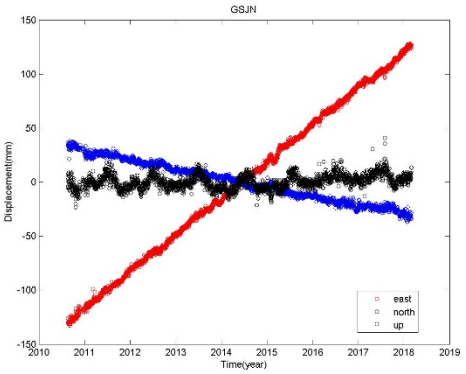
GSJN
Displacement(mm)
Time(year)
east
north
up

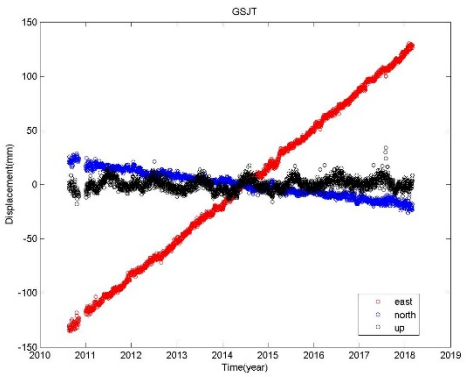
GSJT
Displacement(mm)
Time(year)
east
north
up

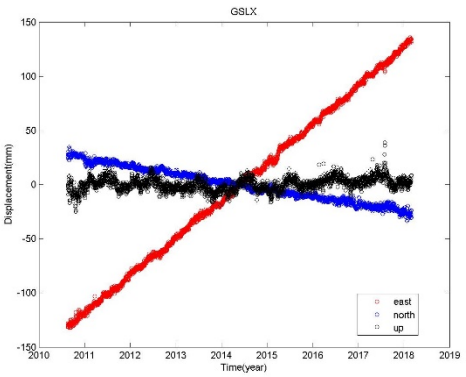
GSLX
Displacement(mm)
Time(year)
east
north
up

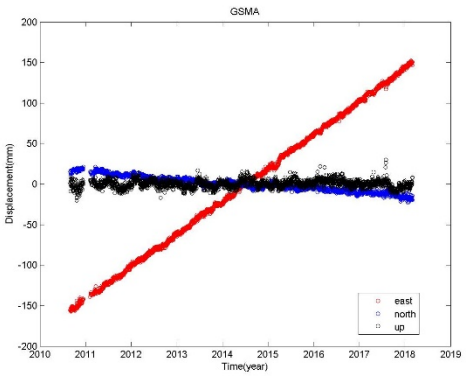
GSMA
Displacement(mm)
Time(year)
east
north
up

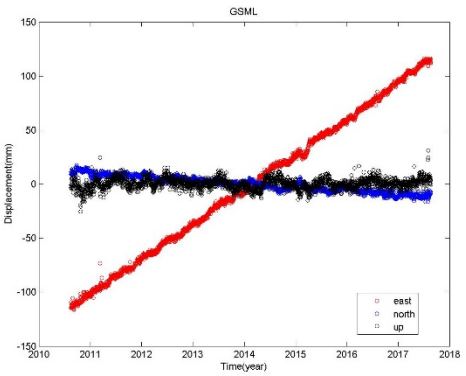
GSML
Displacement(mm)
Time(year)
east
north
up

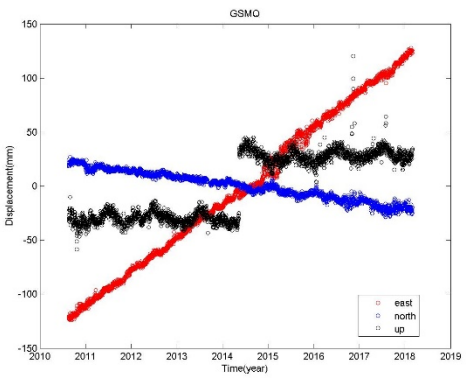
GSMO
Displacement(mm)
Time(year)
east
north
up

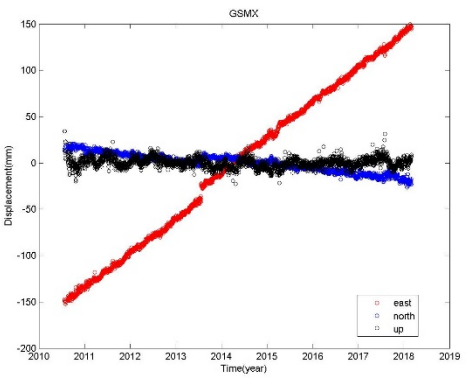
GSMX
Displacement(mm)
Time(year)
east
north
up

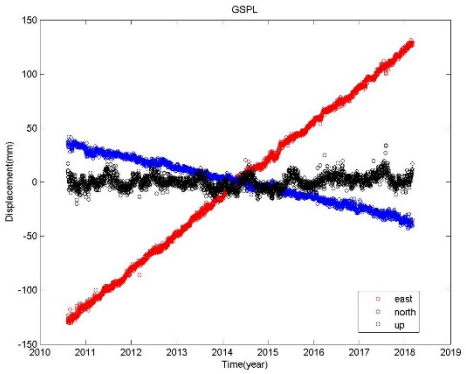
GSPL
Displacement(mm)
Time(year)
east
north
up

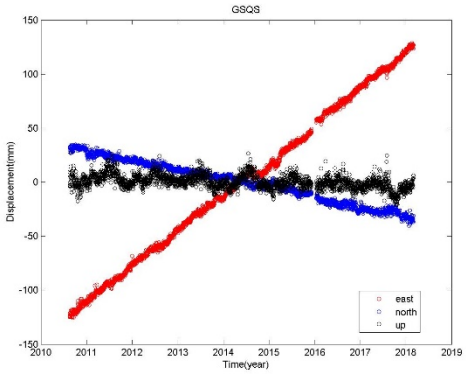
GSQS
Displacement(mm)
Time(year)
east
north
up

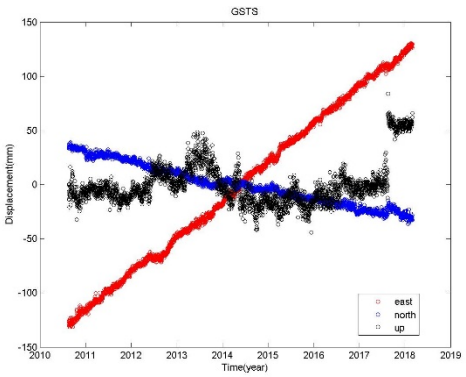
GSTS
Displacement(mm)
Time(year)
east
north
up

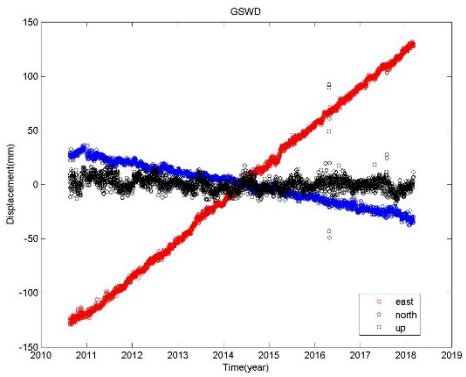
GSWD
Displacement(mm)
Time(year)
east
north
up

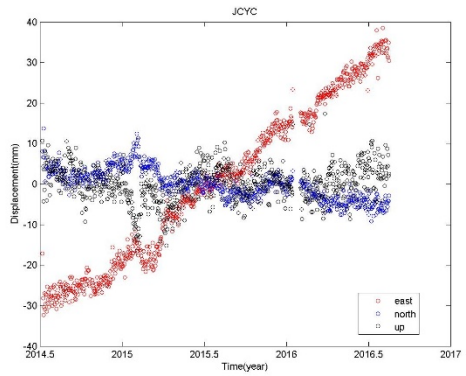
JCYC
Displacement(mm)
Time(year)
east
north
up

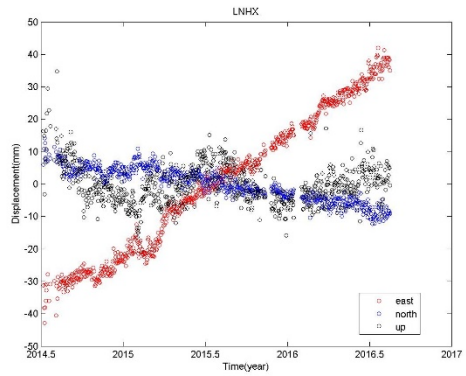
LNHX
Displacement(mm)
Time(year)
east
north
up

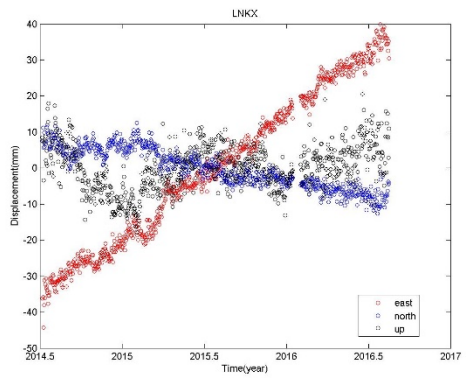
LNKX
Displacement(mm)
Time(year)
east
north
up

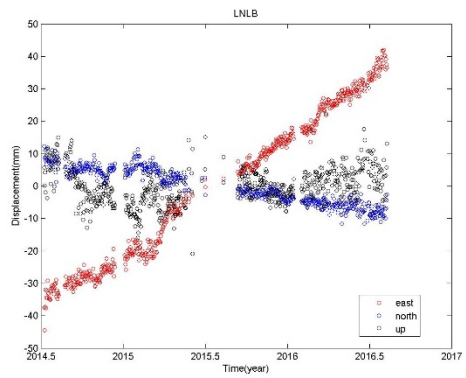
LNLB
Displacement(mm)
Time(year)
east
north
up

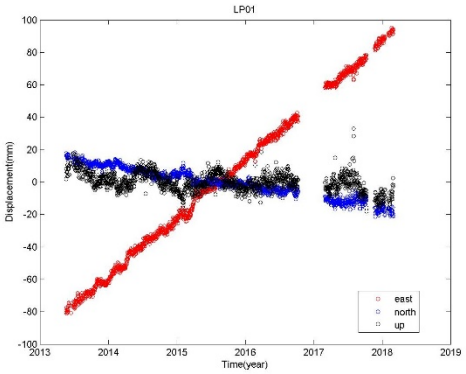
LP01
Displacement(mm)
Time(year)
east
north
up

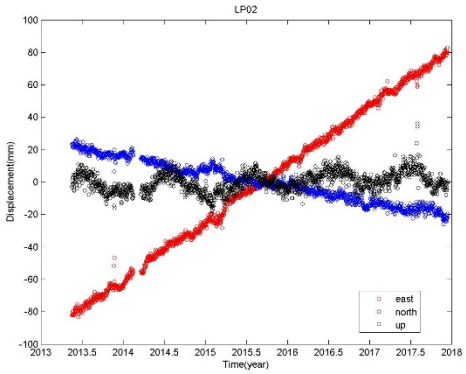
LP02
Displacement(mm)
Time(year)
east
north
up

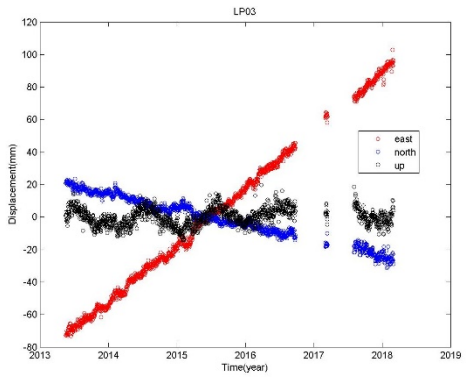
LP03
Displacement(mm)
Time(year)
east
north
up

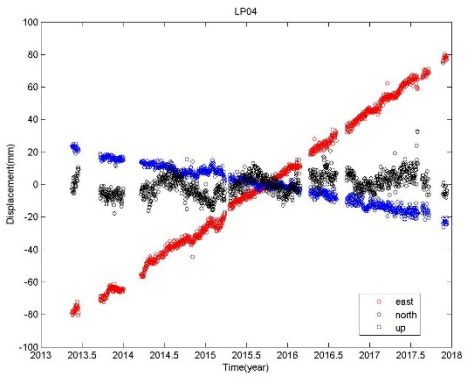
LP04
Displacement(mm)
Time(year)
east
north
up

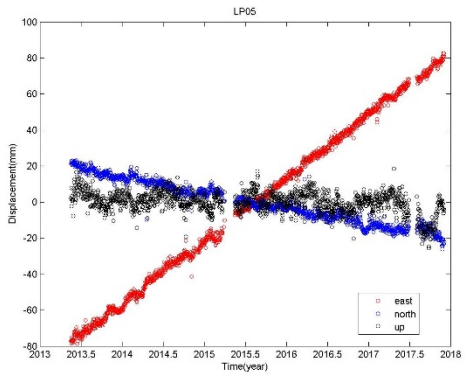
LP05
Displacement(mm)
Time(year)
east
north
up

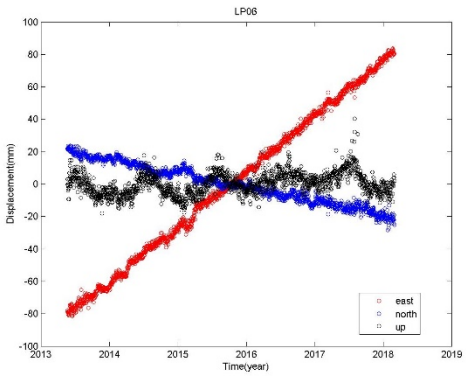
LP06
Displacement(mm)
Time(year)
east
north
up

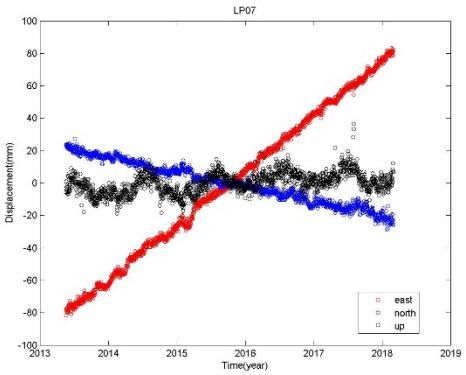
LP07
Displacement(mm)
Time(year)
east
north
up

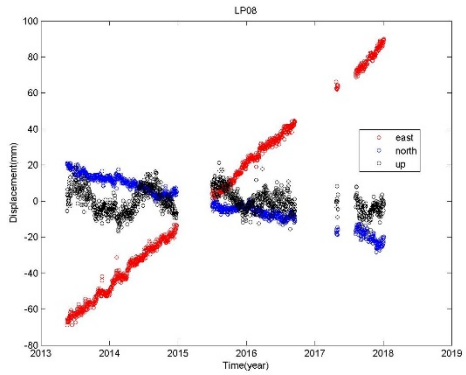
LP08
Displacement(mm)
Time(year)
east
north
up

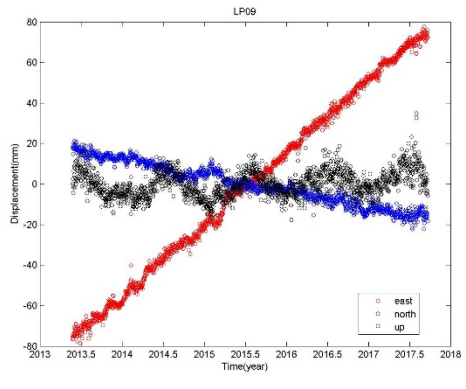
LP09
Displacement(mm)
Time(year)
east
north
up

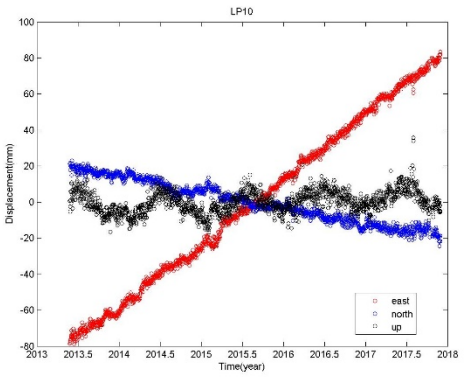
LP10
Displacement(mm)
Time(year)
east
north
up

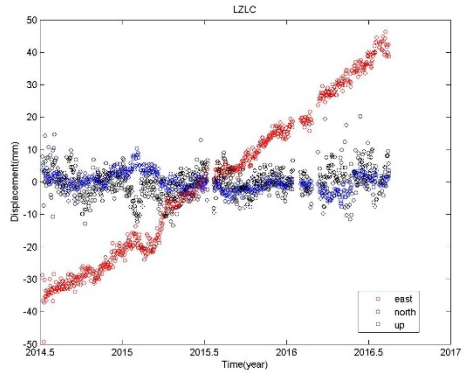
LZLC
Displacement(mm)
Time(year)
east
north
up

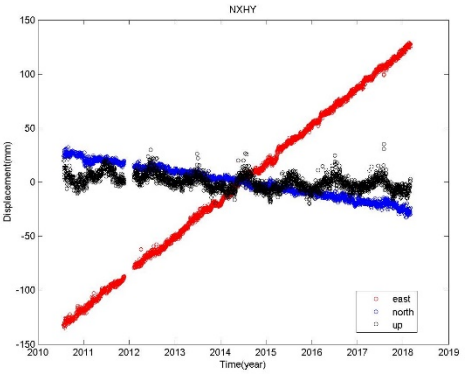
NXHY
Displacement(mm)
Time(year)
east
north
up

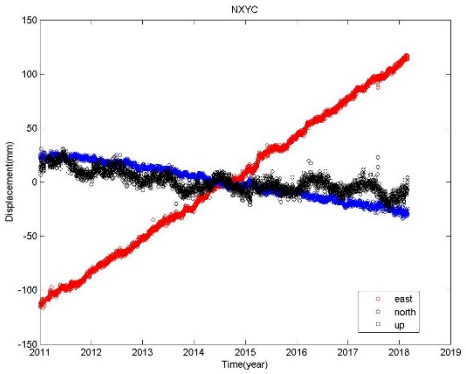
NXYC
Displacement(mm)
Time(year)
east
north
up

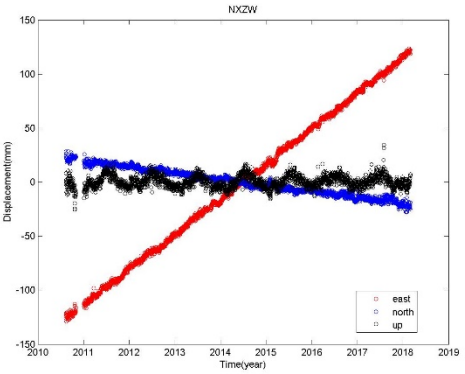
NXZW
Displacement(mm)
Time(year)
east
north
up

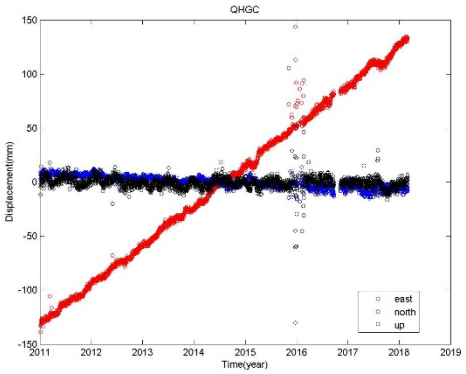
QHGC
Displacement(mm)
Time(year)
east
north
up

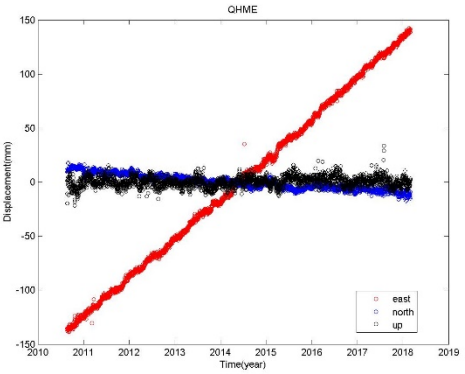
QHME
Displacement(mm)
Time(year)
east
north
up

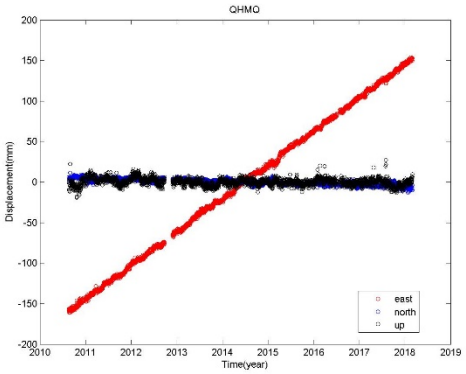
QHMQ
Displacement(mm)
Time(year)
east
north
up

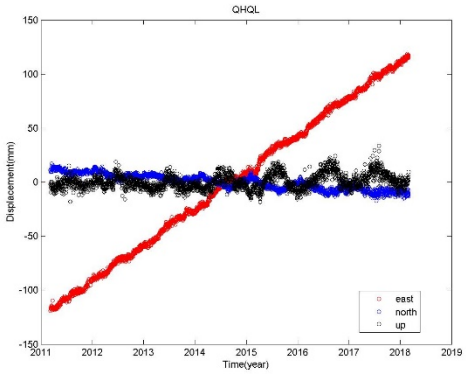
QHQL
Displacement(mm)
Time(year)
east
north
up

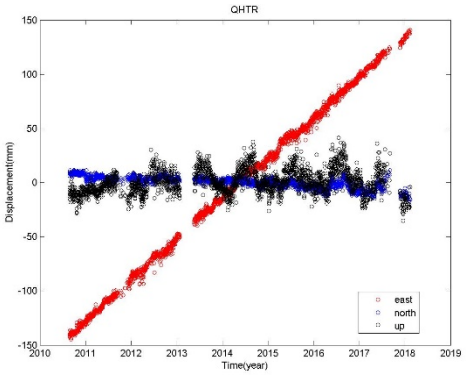
QHTR
Displacement(mm)
Time(year)
east
north
up

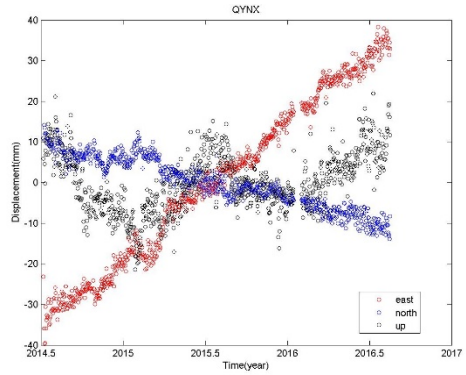
QYNX
Displacement(mm)
Time(year)
east
north
up

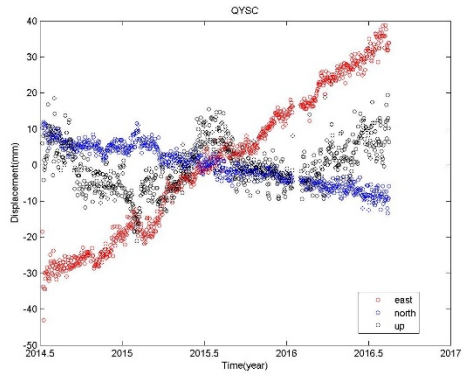
QYSC
Displacement(mm)
Time(year)
east
north
up

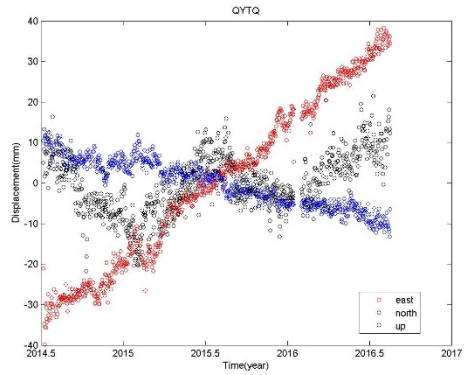
QYTQ
Displacement(mm)
Time(year)
east
north
up

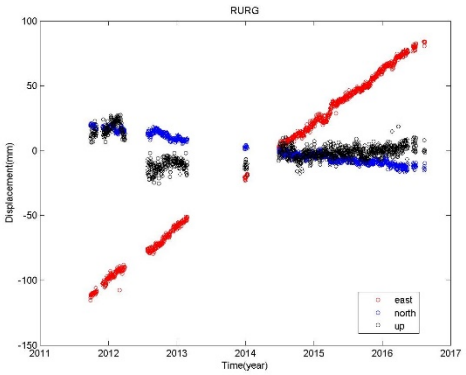
RURG
Displacement(mm)
Time(year)
east
north
up

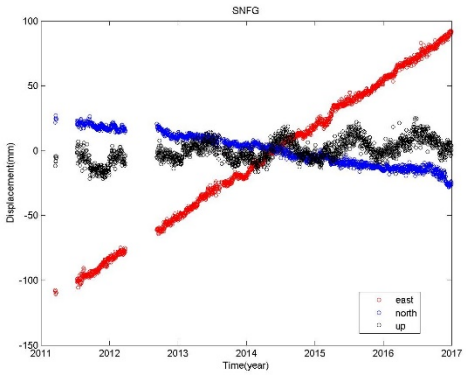
SNFG
Displacement(mm)
Time(year)
east
north
up

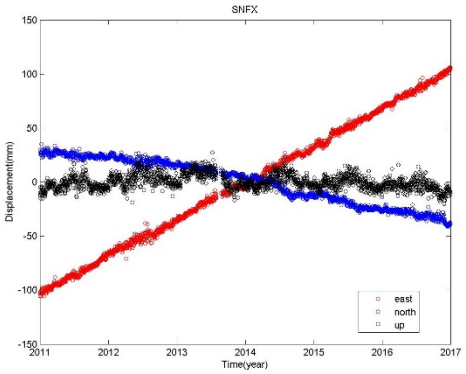
SNFX
Displacement(mm)
Time(year)
east
north
up

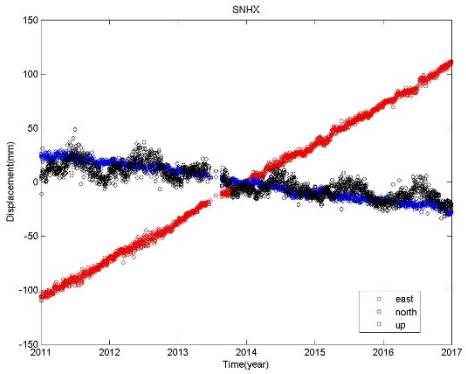
SNHX
Displacement(mm)
Time(year)
east
north
up

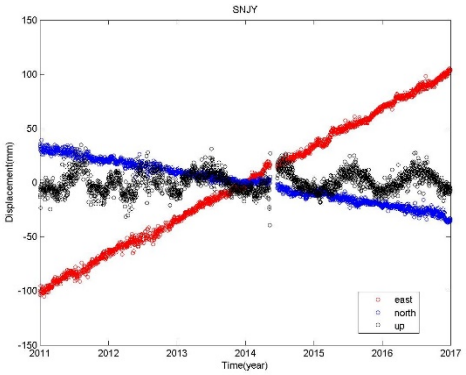
SNJY
Displacement(mm)
Time(year)
east
north
up

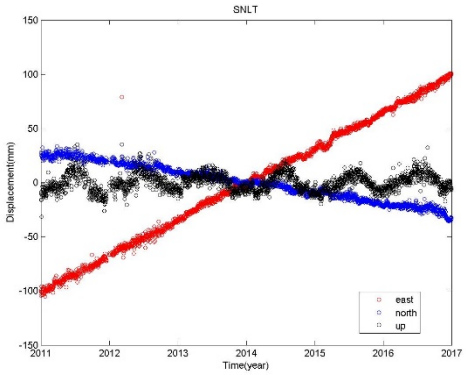
SNLT
Displacement(mm)
Time(year)
east
north
up

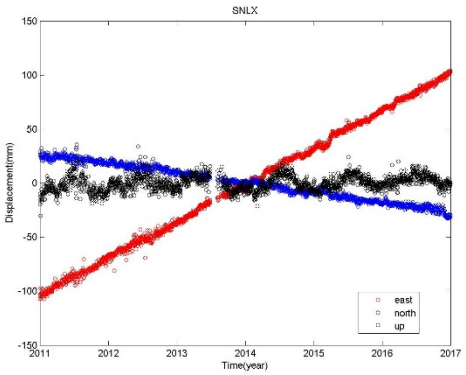
SNLX
Displacement(mm)
Time(year)
east
north
up

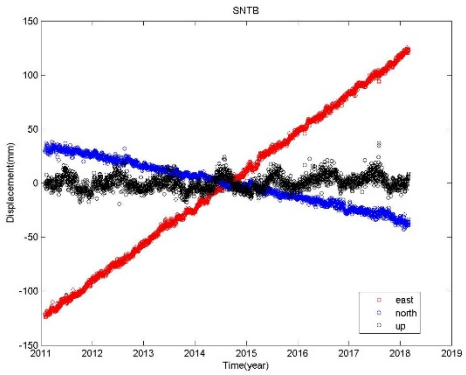
SNTB
Displacement(mm)
Time(year)
east
north
up

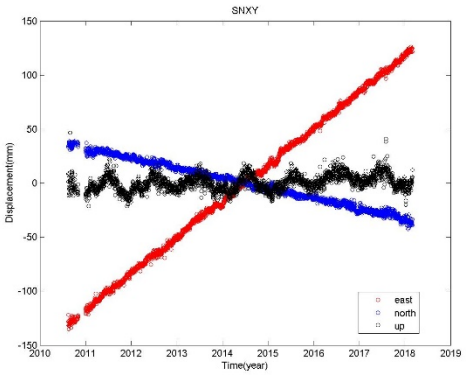
SNXY
Displacement(mm)
Time(year)
east
north
up

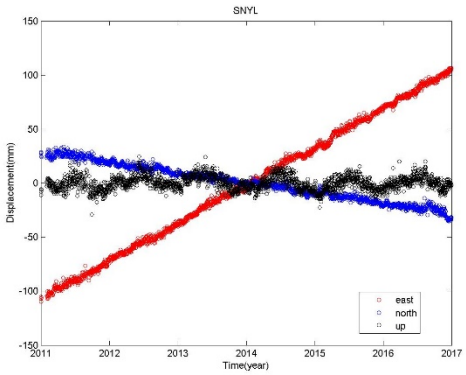
SNYL
Displacement(mm)
Time(year)
east
north
up

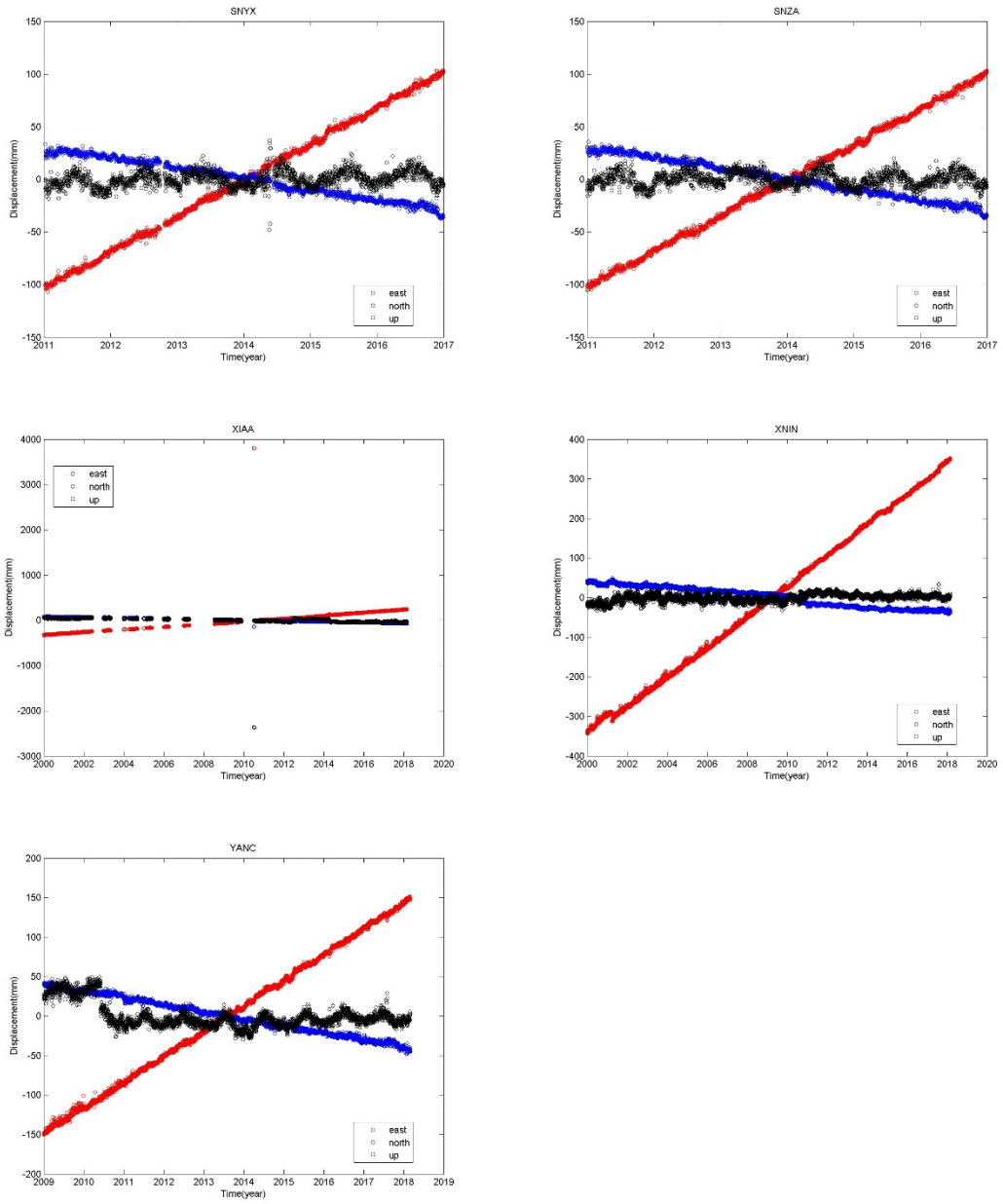

Figure S1. The position time series of 58 cGPS stations relative to ITRF 2014 reference frame.